CHEMICAL ENGINEERING TRANSACTIONS
VOL. 114, 2024
A publication of AIDIC
The Italian Association of Chemical Engineering
Online at www.cetjournal.it
Guest Editors: Petar S. Varbanov, Min Zeng, Yee Van Fan, Xuechao Wang

**ISBN** 979-12-81206-12-0; **ISSN** 2283-9216
DOI: 10.3303/CET24114067

# Evaluation of Enhanced Heat Transfer Condensation in Hydrophobic Tubes

David J. Kukulka[a]*, Rick Smith[b] , Wei Li[c]

[a]State University of New York College at Buffalo, 1300 Elmwood Avenue, Buffalo, New York, 14222 USA,
[b]Vipertex, 658 Ohio Street, Buffalo, New York. USA
[c]Department of Energy Engineering, Zhejiang University, 866 Yuhangtang Road, Hangzhou 310027, China
kukulkdj@buffalostate.edu

Condensation heat transfer performance was studied experimentally in horizontal, stainless-steel (type 304) tubes. This study experimentally studied the effect of hydrophobicity on condensation heat transfer by comparing heat transfer performance of smooth tubes (ST), hydrophobic tubes (HYD), herringbone tubes (HB), and hydrophobic/ herringbone composite tubes (HYD/HB). All tubes had an outer diameter of 12.7 mm; with saturation temperatures of 35 °C and 45 °C; for mass flow rates of 100 kg/($m^2$·s) and 150 kg/($m^2$·s); for refrigerant quality that ranged from 0.2 to 0.9. Performance data that varied with mass flow indicate that the HB tube exhibits superior heat transfer performance when compared to the HYD tube. However, for constant mass flow rate and increasing refrigerant quality, the heat transfer coefficient (h) of the HYD tube increases gradually; at a quality of 0.6, the HYD tube outperforms the HB tube. The physical properties of refrigerant R32 are better (promoting higher h values) at a saturation temperature of 35°C than at 45°C; all the tube types show an improvement in h of approximately 15% at 35°C compared to performance at 45°C. Finally, as the mass flow rate increases, the heat transfer coefficient of the HYD tube improves by about 20% compared to a smooth tube. This improvement is due to the hydrophobic structure, which causes droplet condensation on the inner surface of the tube, increasing the droplet detachment rate and enhancing heat transfer. As the mass flow rate increases, the heat transfer coefficient (h) of the HB tube increases, while those of the HYD/HB tube decrease slightly. This can be explained by the hydrophobic structure of the HB tube; this inhibits the induction of droplets by the herringbone fin; however, the hydrophobic structure is not sufficient to balance this weakening. The HYD tube shows an increasing trend for h as the vapor mass flow increases. This occurs when the refrigerant gas phase dominates over the liquid phase; this prevents the formation of a liquid film forming (from the large droplets produced by the hydrophobic structure). As a result, there is a significant increase in h at an average quality of 0.5; for these conditions the HYD tube outperforms the HB tube and the h of the HYD tube is approximately 20% higher than that of the smooth tube.

## 1. Introduction

Increasing energy use and the production of greenhouse gases (as the result of using many sources of energy) has created environmental problems that must be addressed in present and future designs. Carbon neutrality is an important goal when considering energy use; countries are exploring ways to optimize energy and minimize carbon use. In order to sustain the development of today's world, the conservation of energy is needed. As discussed in Kapustenko et al. (2023), developed countries dominate the emission of carbon dioxide in the area of energy production/ use with thermal power generation responsible for the highest carbon dioxide production. Enhancing heat transfer and increasing the efficiency of heat exchangers are essential in trying to achieve carbon-neutral designs. Several previous studies have explored ways of enhancing the surface structure of a heat transfer surface in order to produce more energy, however few looked at hydrophobic surfaces. With the recent development of enhanced three-dimensional tubes, studies of condensation have become important topics to study. Li et al. (2017) evaluated the condensation heat transfer characteristics in micro finned tubes and compared performance with smooth tubes. Kukulka et al. (2016) experimentally

Paper Received: 12 July 2024; Revised: 21 August 2024; Accepted: 23 November 2024
Please cite this article as: Kukulka D.J., Smith R., Li W., 2024, Evaluation of Enhanced Heat Transfer Condensation in Hydrophobic Tubes, Chemical Engineering Transactions, 114, 397-402 DOI:10.3303/CET24114067

evaluated tube side condensation heat transfer for various enhanced tubes; Kukulka et al. (2019) presented h and frictional pressure drop data for condensation heat transfer on the outside of enhanced three-dimensional tubes. Li et al. **Error! Reference source not found.** compared the heat transfer performance of several stainless-steel enhanced tubes. Additionally, Kukulka et al. (2022) presented visual flow patterns and heat transfer performance for flow condensation under a variety of conditions. Gu et al. (2020) evaluated experimentally the condensation heat transfer of moist air on the outside of three-dimensional finned tubes. Tang et al. (2020) compared the condensation flow patterns found in a three-dimensional enhanced tube and detailed the transition position.

Condensing heat exchangers are widely used in air conditioning systems and typically the most effective way to enhance condensation is to thin the liquid film that is on the heat transfer surface; a variety of passive methods are used to enhance heat transfer including: (i) rough heat transfer surfaces, (ii) extended surfaces, (iii) embedded enhancement devices, (iv) enhancement coils and (v) fluid additives. Use of a hydrophobic surface is an important method to consider in order to enhance droplet condensation designs, these designs produce a low free energy surface. Rykaczewski et al. (2012) investigated the process of droplet formation on nanostructured superhydrophobic surfaces and proposed a model that quantitatively describes the growth of droplets. Currently, there have been relatively few studies conducted on hydrophobic-enhanced composite structures. In their study, Yao et al. (2014) established a hydrophobic-hydrophilic hybrid surface with micro arrays; this was a part of their study on wetting behavior. Experimental results showed that the micropillar spacing ratio was a key factor affecting the results of droplet condensation on the hybrid surface. When the spacing between the micropillars was less than 50 μm, the droplets that had aggregated were dislodged from the surface. However, when the spacing between the micropillars was approximately 50 μm, the agglomerated droplets filled the valleys of the mixed surfaces and formed a thin liquid film. Egab et al. (2020) compared the effect of hybrid wettability on the enhancement of film and droplet condensation. This thin liquid film reduces thermal resistance and increases the condensation rate.

Modifying the surface structure of a tube is a passive enhancement method that requires additional study. For many areas there is a lack of knowledge regarding the performance of hydrophobic surfaces; in order to produce efficient designs an experimental performance analysis must take place to obtain that information. It is impossible to rely solely on a theoretical analysis or a numerical analysis in order to optimize a design with these novel surfaces. Results of this experimental study are important to obtain for a variety of conditions (for variations in mass flow rate and refrigerant quality) in order to determine the thermal performance of these unique tubes.

## 2. Experimental Details

Figure 1 details the experimental apparatus used in this study. Images of the enhanced surfaces studied here are presented in Figure 2. When tube side condensation is studied, the test section (as can be seen in Figure 1) of the apparatus is composed of a horizontal counter-flow heat exchanger; refrigerant flows in the enhanced tube being evaluated, and cooling water is flowing in the external annular casing of the enhanced tube. After the test section, the cooling water is measured using a mass flowmeter and returned to the constant temperature water tank; here, the temperature is measured using a Pt100 platinum resistance temperature sensor. The refrigerant is heated to a predetermined temperature and quality before it enters the test section. In the condenser, the refrigerant flowing from the test section is completely condensed and subcooled. Additional details regarding the experimental setup and procedure are found in Li et al. (2021a, 2021b).

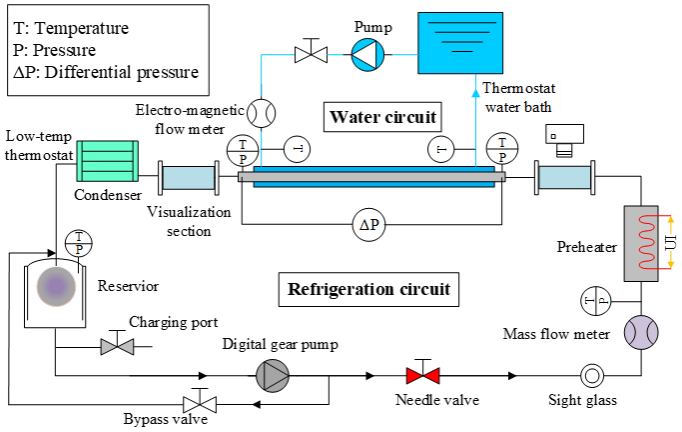


*Figure 1: Schematic of the experimental setup*

Condensation tests were performed at 45 °C (saturation temperature); for mass flux values in the range of 50 to 400 kg/($m^2$·s); with an inlet vapor quality of 0.8 and outlet vapor quality of 0.2. Each test point is repeated three times; the deviation between the test data for the three repeated tests is less than 5 %. Moffat (1988) describes how to calculate the uncertainty (%) of directly measured and indirectly obtained parameters; The maximum relative error of the h is calculated to be ± 11.32 %.

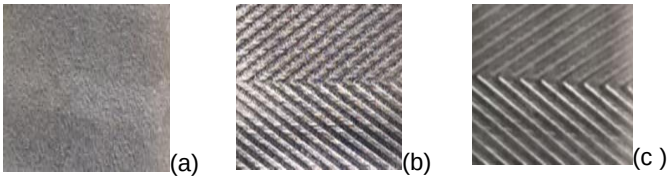


*Figure 2: Images of enhanced surface tubes (a) HYD, (b) HB/HYD, (c) HB*

The current experimental study utilized R32 refrigerant to study enhanced heat transfer tubes [smooth tubes (ST), hydrophobic tubes (HYD), herringbone (HB), and hydrophobic-herringbone (HYD-HB) ] in order to investigate the impact of hydrophobicity and evaluate a hydrophobic-enhanced composite structure. This study lays the foundation for the development of hydrophobic-enhanced composite surfaces.

### 2.1 Tube Details

In this study of the impact of hydrophobicity on condensation heat transfer of smooth (ST) tubes, hydrophobic (HYD) tubes, herringbone (HB) tubes, and hydrophobic herringbone (HYD/HB) tubes were studied. It is important to note that the HYD surface used in this study is not a coating, but it is produced in the material of the tube. Wetting analysis revealed contact angles of 107.35° for the HYD tubes, 48.23° for the HB tubes, and 53.37° for the HYD-HB tubes. Images of these enhanced tubes are given in **Error! Reference source not found.**. All three tube types are constructed from stainless steel, with an outer diameter of 12.7 mm and inner diameter of 11.5 mm. Details of the herringbone structure include: fin height of 0.052 mm; distance between fins of 0.636 mm; and a spiral angle of 18°. Table 1 provides measured quantities and parameters of the various tubes.

*Table 1: Parameters of the enhanced tubes*

| Parameter | ST tube | HB tube | HYD tube | HB/HYD tube |
|---|---|---|---|---|
| Material | Type 304 Stainless steel | Type 304 Stainless steel | Type 304 Stainless steel | Type 304 Stainless steel |
| Inner diameter (mm) | 11.5 | 11.5 | 11.5 | 11.5 |
| Outer diameter (mm) | 12.7 | 12.7 | 12.7 | 12.7 |
| Thickness (mm) | 0.61 | 0.61 | 0.61 | 0.61 |
| Length (mm) | 1.7 | 1.7 | 1.7 | 1.7 |
| fin height (mm) | - | 0.052 | - | 0.052 |
| fin pitch (mm) | - | 0.636 | - | 0.636 |
| Helix angle (°) | - | 18 | - | 18 |
| Addendum angle (°) | - | 161.4 | - | 161.4 |

## 3. Results

### 3.1 Effect of supercooling on hydrophobicity

During the experiment, the subcooling temperature difference ($\Delta T_{sub}$) cannot be directly measured but it can be calculated from equation **Error! Reference source not found.** :

$$\Delta T_{sub} = T_{sat} - T_w = \frac{Q}{U \times A_o} \quad (1)$$

Figure 3 illustrates the variation in heat transfer coefficient at differences in subcooling temperatures for the ST and HYD tubes. As the subcooling temperature difference increases, the growth trend of the heat transfer coefficient gradually slows down; this trend is more pronounced at the saturation temperature of 45℃. This demonstrates that an increase in subcooling temperature (i) impacts the detachment rate of the liquid (ii) increases droplet accumulation (iii) leads to thicker liquid film (iv) increases thermal resistance of the upper wall surface in the microchannel; and (v) weakens the heat transfer effect. The saturation temperature of the ST tube at 35℃ shows the opposite trend. This is due to the smooth surface of the ST tube; it lacks an enhanced surface

and is less affected by the supercooling temperature. In Figure 3, the slope of the curve (for a saturation temperature of 45℃ ) is shallow; the curve shape is the result of the physical properties of the refrigerant. The trend of the HB tube and HYD/HB tube indicates that the herringbone fin structure of the HB tube strengthens the liquid discharge ability; and the subcooling temperature has little effect on it. The composite structure of the HYD/HB tube tends to increase the condensation heat transfer coefficient of the hydrophobic tube; the herringbone-hydrophobic composite tube (with an increase in the subcooling temperature) will gradually be reduced. However, for the saturation temperature of 35°C, the opposite is true, this is due to the effect of the refrigerant properties; R32's physical properties (thermal conductivity, density, surface tension, latent heat of vaporization) at the saturation temperature of 35 ℃ produce a thin liquid layer near the heat transfer surface and produces a lower thermal resistance than that produced at 45 ℃; this moderates the effect that the subcooling temperature has on heat transfer.

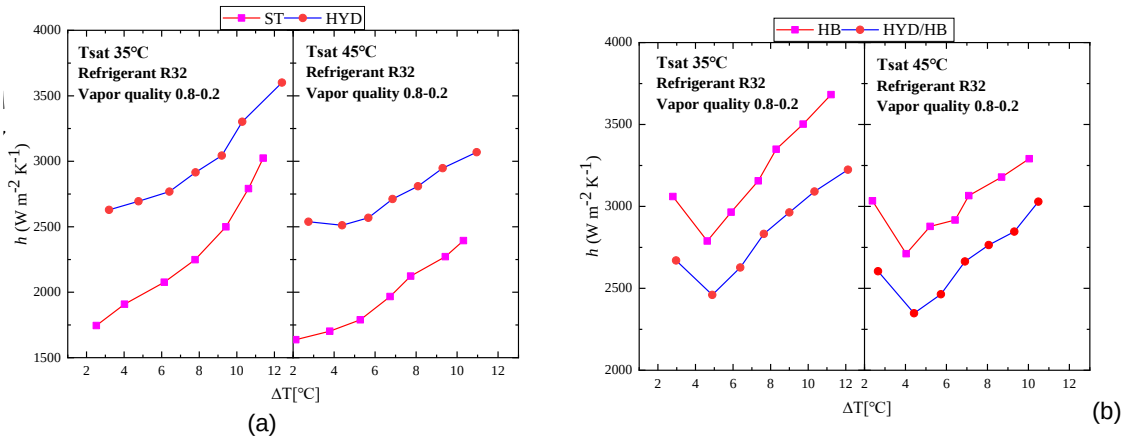


*Figure 3: Effect of subcooling temperature difference on heat transfer coefficient (a) Smooth tube and HYD tube (b) HB tube and HYD/HB tube*

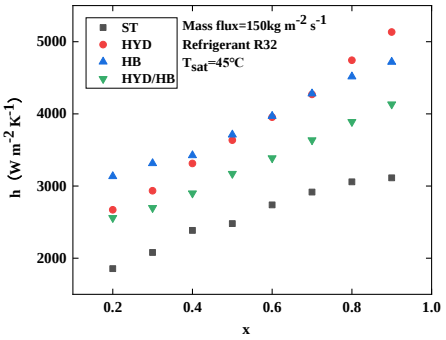


*Figure 4: Condensation heat transfer coefficient as a function of quality for various enhanced surface tubes*

### 3.2 Effect of vapor mass percentage on condensing heat transfer

Figure 4**Error! Reference source not found.** compares the effect of quality on the heat transfer coefficient, it can be seen that the heat transfer coefficient shows a positive correlation with increasing quality for an increase in channel gas-phase refrigerant and a decrease in liquid-phase refrigerant. This cuts down on the liquid-phase refrigerant on the wall surface of the liquid film (this is caused by the thinning of the liquid film); for qualities in the range from 0.2 ~ 0.5 the heat transfer performance of the herringbone tube is higher than the performance of the hydrophobic tube. In the quality range of 0.6 ~ 0.7 the heat transfer coefficient (h) of the tubes are approximately the same; as the quality increases over approximately 0.7 the h of the hydrophobic tube becomes progressively higher than the h of the herringbone tube. When the quality reaches 0.6, the hydrophobic structure produces microchannel droplet detachment as a result of continued detachment and generation; this produces the full exchange of heat and produces the trend shown in Figure 4 **Error! Reference source not found.**.

### 3.3 Effect of mass flow rate on hydrophobicity

**Error! Reference source not found.**Figure 5 shows that the heat transfer coefficients of the four tubes are higher at a saturation temperature of 35°C than at 45°C. Li et al. (2023) presents a detailed discussion that explains how the physical parameters (latent heat of vaporization, surface tension, thermal conductivity of the liquid, vapor density, and vapor kinetic viscosity) of refrigerant R32 produce a higher h at 35°C when compared to 45°C. To analyze the effect of hydrophobicity, the ST tube is compared with a hydrophobic, herringbone and herringbone hydrophobic composite tube. The heat transfer coefficient of the HYD tube is approximately 20% higher than that of the ST tube. This is because the hydrophobic structure modifies the upper wall surface of the tube with a lower surface free energy, preventing the refrigerant from generating a liquid film on the upper wall surface. Due to the increase in contact angle, the upper wall surface of the tube forms large and small droplets, resulting in a droplet condensation flow pattern. As the mass flow rate increases, the ability of the droplet to detach increases; this accelerates the rate of droplet formation on the condensation wall surface and increases heat transfer. The rate of droplet formation on the condensing wall surface is accelerated and enhances heat transfer capability by the rapid removal of heat. According to Li et al. (2023), the HB tube fin effect is larger than the fin effect in the HYD/HB tube since the hydrophobic structure is preventing the herringbone fin structure from inducing droplets. More specifically, the hydrophobic structure continuously forms droplets on its surface and the herringbone finned-based structure causes the droplets to coalesce in the grooves; this leads to the enlargement of droplets and increased thermal resistance of the condensing surface. This produces a smaller condensation heat transfer coefficient.

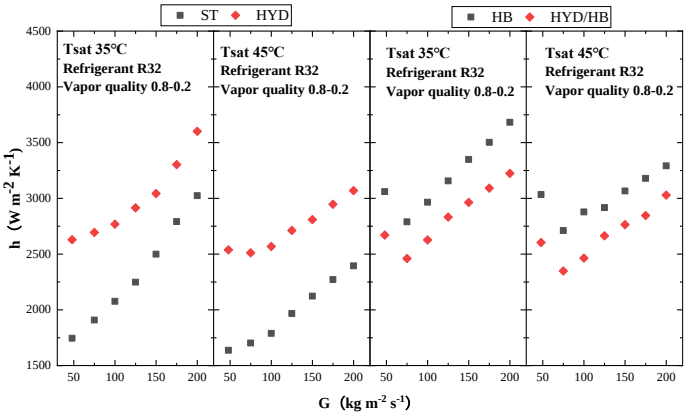


*Figure 5: Variation of the heat transfer coefficient with mass flow rate for tubes (ST and HYD) and (HB and HYD/HB)*

## 4. Conclusions

In order to assess the impact of the hydrophobic structure on tube side condensation heat transfer, an experiment was performed that collected 90 data points over four different scenarios using refrigerant R32. Conditions included saturation temperatures being set at $T_{sat}$=35°C and $T_{sat}$=45°C; with mass flow rates of 100 kg $m^{-2}$ $s^{-1}$ and 150 kg $m^{-2}$ $s^{-1}$. Specific conclusions derived from this analysis are as follows:

--The physical characteristics of refrigerant R32 exhibit superior performance at a saturation temperature of $T_{sat}$=35°C when compared to the performance at $T_{sat}$=45°C. Consequently, all four tube types demonstrate an enhancement of approximately 15% at $T_{sat}$=35°C when compared to performance at $T_{sat}$=45°C. Moreover, as the mass flow rate increases, the heat transfer coefficient of the HYD tube increases by approximately 20% (when compared to a smooth tube). This enhancement is attributed to the hydrophobic structure, which promotes droplet condensation on the inner surface of the tube; this increases the droplet detachment rate and increases the heat transfer efficiency.

--As the mass flow rate increases, the heat transfer coefficients of the HB tube increases, while that of the HYD/HB tube decreases by about 5%. This can be explained by the hydrophobic structure of the HB tube; this structure inhibits the induction of droplets by the herringbone fin. However, the hydrophobic structure is not sufficient to balance this weakening.

--Performance of the HYD tube increases by approximately 20% as the vapor mass flow rate increases. This occurs when the refrigerant gas phase dominates over the liquid phase; this prevents the formation of a liquid film from the large droplets produced by the hydrophobic structure. As a result, there is a significant increase at an average vapor mass flow rate for a quality of 0.5; here the HYD surface surpasses the HB tube.

**Nomenclature**

| | |
|---|---|
| $A_o$ | Outer area, $m^2$ |
| G | Mass flux, kg $m^{-2}$ $s^{-1}$ |
| Q | Heat flow rate, $W/m^2$ |
| T | Temperature, °C/K |
| U | Total heat transfer coefficient, W / ($m^2$ K) |
| h | Heat transfer coefficient, W / ($m^2$ K) |
| x | Quality |

**Subscripts**

| | |
|---|---|
| w | Water |
| sat | Saturation |

**References**


Egab K., Alwazzan M.J., Peng B., Oudah S.K., Guo Z., Dai X., Khan J.A., Li C.,2020, Enhancing filmwise and dropwise condensation using a hybrid wettability contrast mechanism: Circular patterns. Int J Heat Mass Tran, 154(1),19640.

Gu Y., Liu Q., Cheng M., Ding Y., Zhu X., 2020, Condensation heat transfer characteristics of moist air outside a three-dimensional finned tube. Int J Heat Mass Transfer,158,119983.

Kapustenko P., Klemeš J.J., Arsenyeva, O., 2023, Plate heat exchangers fouling mitigation effects in heating of water solutions: A review. Renewable & Sustainable Energy Reviews,179, 113283.

Kukulka D.J., Smith R., Li W. , 2016, Comparison of condensation and evaporation heat transfer on the outside of smooth and enhanced 1EHT tubes. Appl Therm Eng, 105, 913–22.

Kukulka D.J., Smith R., Li W., 2019, Experimental Comparison of the Evaporation and Condensation Heat Transfer Coefficients on the Outside of Enhanced Surface Tubes with Different Outer Diameters. Chemical Engineering Transactions ,76, 3136.

Kukulka D.J., Smith R., Li W., 2022, Heat Transfer Performance of Microfin Tubes and Three-Dimensional Heat Transfer Tubes. Chemical Engineering Transactions, 94, 265-70.

Li W., Tang W., Gu Z., Guo Y., Ma X., Minkowycz W.J., He Y., Kukulka D.J. , 2020, Analysis of condensation and evaporation heat transfer inside 3-D enhanced tubes. Numerical Heat Transfer Part A-applications, 78(10), 525–40.

Li G., Huang L., Tao L., 2017, Experimental investigation of refrigerant condensation heat transfer characteristics in the horizontal microfin tubes. Appl Therm Eng, 123,1484-93.

Li W., Wang J., Guo Y., Shi Q., He Y., Kukulka D.J., Luo X., Kabelac S., 2022, R410A flow condensation inside two dimensional micro-fin tubes and three dimensional dimple tubes. International Journal of Heat and Mass Transfer,182,121910.

Li W., Wang J., Guo Y., Gu Z., Wang X., Sun Z., Tang W., Kukulka D.J., 2021, Two-phase heat transfer of R410A in annuli outside enhanced tubes with micro-fin and dimple. International Journal of Heat and Mass Transfer,175,121370.

Li W., Feng W., Liu X., Li J., Cao B., Dou B., Zhang J., Kukulka D.J.,2023, Condensation heat transfer and pressure drop characteristics inside smooth and enhanced tubes with R410A and R32. Int J Heat Mass Tran, 214, 124419.

Moffat R.J., 1988, Describing the uncertainties in experimental results. Experimental Thermal and Fluid Science,1(1), 3–17.

Rykaczewski K., 2012, Microdroplet Growth Mechanism during Water Condensation on Superhydrophobic Surfaces. Langmuir, 28(20), 7720–29.

Tang W., Sun Z., Li W., 2020, Visualization of flow patterns during condensation in dimpled surface tubes of different materials. Int J Heat Mass Tran,161,120251.

Yao C., Alvarado J.L., Marsh C., Jones B.C., Collins M.K., 2014, Wetting behavior on hybrid surfaces with hydrophobic and hydrophilic properties. Applied Surface Science, 290,59–65.